Gravitational waves from preheating in M-flation

JCAP03(2014)020

(http://iopscience.iop.org/1475-7516/2014/03/020)

Journal of Cosmology and Astroparticle Physics
An IOP and SISSA journal

Gravitational waves from preheating in M-flation

Amjad Ashoorioon,[a] **Brandon Fung,**[b] **Robert B. Mann,**[b,c] **Marius Oltean**[d] **and M.M. Sheikh-Jabbari**[e,f]

[a]Physics Department, Lancaster University, Lancaster, LA1 4YB, United Kingdom
[b]Department of Physics and Astronomy, University of Waterloo, 200 University Avenue, Waterloo, Ontario, N2L 3G1, Canada
[c]Perimeter Institute for Theoretical Physics, 35 Caroline St., Waterloo, Ontario, N2L 2Y5, Canada
[d]Department of Physics, McGill University, Montréal, Québec, H3A 2T8, Canada
[e]School of Physics, Institute for Research in Fundamental Sciences (IPM), Tehran, Iran
[f]Department of Physics, Kyung Hee University, Seoul 130-701, Korea
E-mail: a.ashoorioon@lancaster.ac.uk, b6fung@uwaterloo.ca, rbmann@uwaterloo.ca, moltean@physics.mcgill.ca, jabbari@theory.ipm.ac.ir

Received January 11, 2014
Accepted February 11, 2014
Published March 12, 2014

Abstract. Matrix inflation, or M-flation, is a string theory motivated inflationary model with three scalar field matrices and gauge fields in the adjoint representation of the $\mathbf{U}(N)$ gauge group. One of these $3N^2$ scalars appears as the effective inflaton while the rest of the fields (scalar and gauge fields) can play the role of isocurvature fields during inflation and preheat fields afterwards. There is a region in parameter space and initial field values, "the hilltop region," where predictions of the model are quite compatible with the recent *Planck* data. We show that in this hilltop region, if the inflaton ends up in the supersymmetric vacuum, the model can have an embedded preheating mechanism. Couplings of the preheat modes are related to the inflaton self-couplings and therefore are known from the CMB data. Through lattice simulations performed using a symplectic integrator, we numerically compute the power spectra of gravitational waves produced during the preheating stage following M-flation. The preliminary numerical simulation of the spectrum from multi-preheat fields peaks in the GHz band with an amplitude $\Omega_{\rm gw}h^2 \propto 10^{-16}$, suggesting that the model has concrete predictions for the ultra-high frequency gravity-wave probes. This signature could be used to distinguish the model from rival inflationary models.

Keywords: cosmology with extra dimensions, gravitational waves / theory, inflation, string theory and cosmology

ArXiv ePrint: 1312.2284

doi:10.1088/1475-7516/2014/03/020

JCAP03(2014)020

Contents

1 Introduction

Cosmological observations — evidenced, most notably, by recent data [1] from the *Planck* satellite — are best explained if we have a period of accelerated expansion, inflation [2–4], in the early Universe. Models of inflation usually involve one or more scalar fields coupled to (Einstein) gravity, though it is also possible that inflation is driven by gauge fields [5]. These models are specified by the form of their kinetic terms as well as the potential. It is more common to take the canonical kinetic term and define the model by its potential(s), even though inflationary models can be realized with non-canonical kinetic terms [6].

To explain the observed Universe, inflation should of course end and the energy stored in the inflationary sector should be transferred into the (beyond) Standard Model (SM) particles, an epoch known as the reheating era [2–4, 7]. Perturbative decay of quantum fluctuations of an inflaton field (perturbative reheating) is usually not sufficiently fast and efficient, and leads to reheat temperatures that are too low to solve particle physics problems and hence to describe what we see.[1] One must therefore equip inflationary models with non-perturbative mechanisms of decay that yield sufficiently high reheat temperatures. In this context the inflaton field condensate can provide "time dependent mass terms" for other fields coupled to it, the *preheat* fields. This more efficient energy transfer mechanism to other (beyond Standard Model) fields, preheating, happens because of possible resonance bands [8, 9]. The energy in the preheat fields will eventually equilibrate or thermalize through usual (perturbative) scattering processes [7].

[1] Big Bang Nucleosynthesis (BBN) requires a temperature of order $1 - 10\,\mathrm{MeV}$ and baryogenesis requires a temperature of order $1 - 10\,\mathrm{TeV}$. The reheat temperature should be at least bigger than these two temperatures.

JCAP03(2014)020

Observable effects of inflationary models (in particular the observed CMB anisotropy [1]) are usually attributed to what happened during inflation and are related to super-horizon quantum fluctuations of inflaton fields that appear as classical background fluctuations long after inflation, and after the preheating and reheating eras [2–4]. The CMB data have hence been used to restrict inflationary models [1]. However the recent *Planck* mission data — in particular non-observation of non-Gaussianity — means that the CMB data does not provide sufficient constraints to specify the inflaton potential. Other sources of cosmic data must be sought out.

To this end, a more concrete understanding/modelling of reheating and preheating may be needed. Various inflationary models can be constrained by probing possible specific features they left during preheating or reheating. Previous analysis indicates that preheating may have detectable traces on CMB only for a specific class of exotic models [10–12]. If preheating occurs the turbulent, explosive and non-thermal energy transfer to the preheat sector can in principle have possible observable effects by producing a stochastic background of gravity waves typically in $10^7 - 10^9$ Hz frequency band[2] [15, 16].

The simplest scalar-driven slow-roll models (in particular, those with concave potentials[3]) have so far passed the test very well insofar as *Planck* results are concerned, see e.g. [19]. Nevertheless there remain with these models a plethora of unresolved theoretical difficulties [20]. For instance, to have successful slow-roll inflation we need to keep the inflaton mass hierarchically smaller than the Hubble scale H during inflation and quantum corrections to the inflaton potential should not spoil its flatness [21]. Moreover, in the class of large-field models there is also the problem of super-Planckian field excursions: that inflaton(s) in these scalar models typically have field displacements (in the last 60 e-folds) many times larger than $M_{\rm pl}$, in which case quantum (gravity) effects may become important [22].

It is a general belief that these and other theoretical issues regarding possible classical or quantum instabilities in an inflationary model can/should be addressed within a quantum gravity setup that is operative at some high energy (Planckian or sub-Planckian) scale. Despite providing a richer framework for inflationary model building and for addressing the above mentioned issues, being farther from SM physics, it becomes more challenging in the quantum gravity setups to make connections with physics after inflation and in particular to have a successful reheating scenario. Nonetheless, working within a string theoretic perspective, besides providing a framework to address questions about UV stability and completeness of inflationary models, usually brings another feature: there are many more fields besides the inflaton in the model. These fields can appear as isocurvature entropy modes, affecting the CMB directly, or can appear as preheat fields, affecting the production of primordial gravity waves in large frequency bands.

M-flation, which we will consider in this work, is one such model [23]. Although motivated from string theory (quantum gravity) M-flation, as we will show, has the advantage of having an embedded successful preheating mechanism in some regions of parameter space. Furthermore, the model is based on a gauge field theory, the same framework upon which beyond SM models operate, and is thus close to particle physics setups too.

[2]Preheating can also lead to production of long-lived non-linear excitations of the scalar field which dominates the universe and can lead to stochastic gravitational wave background [13].

[3]Note that a choice of non-Bunch-Davies (excited) initial states for the cosmic perturbations can readily change this conclusion [17]. Also if gravity is an inherently a classical theory, there will be no B-mode polarization in the CMB [18].

JCAP03(2014)020

In general and in a string theory/supergravity framework, depending on whether the inflaton field(s) is (are) coming from open string or closed string degrees of freedom, there are two venues for inflationary model building [24, 25]. M-flation, in this sense, is an open string model. However it has its own specific features that may justify viewing it as a third venue. For example, as we will review in section 2, inflation in M-flation is not associated with a mobile brane, unlike all the other known open string models. M-flation is rather motivated by the dynamics of D3-branes subject to a proper RR six-form in a specific ten-dimensional type IIB supergravity background [23]. The inflaton fields of M-flation are three $N \times N$ matrix valued scalar fields associated with the position of a stack of N D3-branes in this background. The action for M-flation, cf. section 2, will hence include U(N) gauge fields (and possibly their spinorial counterparts in a supersymmetric setting). The model is compatible with the *Planck* data if inflation happens in the hilltop $\phi < \mu$ region. In the symmetry breaking region, $\phi > \mu$, the model predicts a large tensor/scalar ratio, $r \simeq 0.2$, which is not compatible with the upper bound of 0.11 with 95% CL if one assumes that the perturbations start from a Bunch-Davies vacuum. The model could be still made compatible with *Planck* if we assume excited initial states for the scalar or tensor fluctuations, as pointed out in [17].

What renders M-flation theoretically appealing is not only its ability to naturally address and resolve the theoretical difficulties of standard inflationary scenarios raised above [26], but also the fact that it can connect to post-inflation physics: it comes with its own built-in preheating mechanism in some regions of parameter space with no extra parameters (compared to the inflationary background sector), and also it has the desirable form of a gauge theory (cf. discussions above).

While work on M-flation has so far been directed more toward exploring it during inflation [23, 26, 27], it is of appreciable importance to also address the question of its possible observable effects coming from its built-in preheating period. In particular, we focus our attention in this paper on gravity waves (GW) produced during the preheating phase following inflation, in some region of parameter space. Their observational signature is revealed by way of their power spectrum, which we numerically compute here with the help of the lattice simulator HLattice 2.0[4] [28].

The rest of this paper is organized as follows. In section 2, we review the basic setup of M-flation. In sections 3 and 4, we describe its embedded preheating mechanism. Then, in section 5, we proceed with computing the power spectra of GW thereby generated. Finally, section 6 presents some concluding remarks.

2 M-flation

Our setting is a 10-dimensional type IIB supergravity background,[5] which is probed by a stack of N D3-branes endowed with Yang-Mills gauge fields. Thus, there exist 6 spatial dimensions perpendicular to the D3-branes, whose positions within this subspace are represented by 6 $N \times N$ matrices. The role of the inflaton, according to the original M-flation setup, is assumed by 3 out of 6 matrix degrees of freedom,[6] which we henceforth denote as $\mathbf{\Phi}_i, i = 1, 2, 3$. The

[4]For an updated version, the software and its user instructions see http://www.cita.utoronto.ca/~zqhuang/hlat/.

[5]For a detailed specification, the reader is referred to section 8 of [23].

[6]We assumed the 6 extra-dimensions are compactified on a CY_3 or T^6 manifold that has two three-cycles, one considerably larger than the other. In principle we can use all 6 extra dimensions and work with 6 matrices, which could be related generators of SO(6) or a subgroup of it.

JCAP03(2014)020

inflaton matrices are, by construction, in the adjoint representation of the $\mathbf{U}(N)$ gauge group; therefore they are non-commutative as well as Hermitian.

In principle, the dynamics of these matrices is very complicated (increasingly so with larger N), as one has any number of possible configurations of the D3-branes within the chosen background. However there is a way to simplify the situation and make it computationally tractable. As we will elaborate in the next subsection, the classical dynamics of this model can be consistently truncated to a solution where the N D3-branes are uniformly distributed along the surface of a 2-sphere (within the 6-dimensional orthogonal subspace), and their positions on this sphere do not change during inflation. What instead changes is the sphere's radius, which thereby plays the role of an effective scalar inflaton.

Aside from the above, many other solutions — that make use of more of the available (classical) degrees of freedom — are of course possible. This possibility was considered in [27] and generically appears as a multi field inflationary model. In this work, however, we focus on the single field model where the other "unused" degrees of freedom in this particular solution will be identified with preheat fields after inflation ends.

2.1 Action and equations of motion

We work in the $(-,+,+,+)$ metric signature, and use boldface to denote matrices of dimension N. The effective $(3+1)$-dimensional action of M-flation [26] comprises Einstein gravity, minimally coupled to a Yang-Mills gauge field $\mathbf{A}_\mu$ and the three inflaton matrices $\mathbf{\Phi}_i$,

$$S = \int \mathrm{d}^4x\sqrt{-g}\left\{\frac{M_{\rm pl}^2}{2}R - \frac{1}{4}\mathrm{Tr}\left(\mathbf{F}_{\mu\nu}\mathbf{F}^{\mu\nu}\right) - \frac{1}{2}\mathrm{Tr}\left(D_\mu\mathbf{\Phi}_i D^\mu\mathbf{\Phi}_i\right) - V\left(\mathbf{\Phi}_i,[\mathbf{\Phi}_j,\mathbf{\Phi}_k]\right)\right\}, \quad (2.1)$$

where, as usual, $M_{\rm pl} = 1/\sqrt{8\pi G}$ is the reduced Planck mass, $\mathbf{F}_{\mu\nu} = 2\partial_{[\mu}\mathbf{A}_{\nu]} + \mathrm{i}g_{\rm YM}[\mathbf{A}_\mu,\mathbf{A}_\nu]$ is the gauge field strength, and $D_\mu = \partial_\mu + \mathrm{i}g_{\rm YM}[\mathbf{A}_\mu,\cdot]$ is the gauge covariant derivative. Moreover, the potential is given by

$$V\left(\mathbf{\Phi}_i,[\mathbf{\Phi}_i,\mathbf{\Phi}_j]\right) = \mathrm{Tr}\left(-\frac{\lambda}{4}[\mathbf{\Phi}_i,\mathbf{\Phi}_j][\mathbf{\Phi}_i,\mathbf{\Phi}_j] + \frac{\mathrm{i}\kappa}{3}\epsilon_{jkl}[\mathbf{\Phi}_k,\mathbf{\Phi}_l]\mathbf{\Phi}_j + \frac{m^2}{2}\mathbf{\Phi}_i\mathbf{\Phi}_i\right), \quad (2.2)$$

where in (2.1) and (2.2) there is a sum on repeated i,j,k indices and the three coupling constants have various stringy meanings: $\lambda = 8\pi g_s = 2g_{\rm YM}^2$ is related to the string coupling g_s, $\kappa = \hat{\kappa}g_s\sqrt{8\pi g_s}$ is related to the Ramond-Ramond antisymmetric form strength $\hat{\kappa}$, and m is a parameter that multiples the three spatial coordinates along the D3-branes in the metric of the background SUGRA theory [23]. To ensure a constant dilaton therein, we must also impose the constraint $\lambda m^2 = 4\kappa^2/9$ [23].

The equations of motion for the scalar and gauge fields that follow from the action (2.1) are

$$D_\mu D^\mu\mathbf{\Phi}_i + \lambda[\mathbf{\Phi}_j,[\mathbf{\Phi}_i,\mathbf{\Phi}_j]] - \mathrm{i}\kappa\epsilon_{ijk}[\mathbf{\Phi}_j,\mathbf{\Phi}_k] - m^2\mathbf{\Phi}_i = 0, \quad (2.3)$$

$$D_\mu\mathbf{F}^{\mu\nu} - \mathrm{i}g_{\rm YM}[\mathbf{\Phi}_i,D^\nu\mathbf{\Phi}_i] = 0. \quad (2.4)$$

2.2 Truncation to the SU(2) sector

The dynamics determined by the equations of motion (2.3) and (2.4) can generically be quite complicated, but this may be simplified considerably as follows. Let $\mathbf{J}_i\,, i = 1,2,3$ denote the

JCAP03(2014)020

three $N \times N$ generators of the $\mathbf{SU}(2)$ algebra, so that $[\mathbf{J}_i, \mathbf{J}_j] = \mathrm{i}\epsilon_{ijk}\mathbf{J}_k$. Now, we decompose the inflaton matrices into two parts,

$$\mathbf{\Phi}_i = \hat{\phi}\mathbf{J}_i + \mathbf{\Psi}_i, \tag{2.5}$$

one parallel and one perpendicular to the $N \times N$ representation of $\mathbf{SU}(2)$, respectively (that is $\mathrm{Tr}(\mathbf{J}_i\mathbf{\Psi_i}) = 0$). It was shown in [23] that if $\mathbf{\Psi}_i = \dot{\mathbf{\Psi}}_i = 0$ initially, then (2.3) implies that $\mathbf{\Psi}_i$ will remain vanishing for all time. Analogously, if $\mathbf{A}_\mu$ is also initially turned off, then the commutator in (2.4) will not source $\mathbf{F}_{\mu\nu}$, and therefore the gauge field always stays turned off as well.

Hence, it is possible to consistently restrict the classical dynamics of this model to a sector where $\mathbf{\Psi}_i = \mathbf{A}_\mu = 0$, so that the inflationary trajectory is determined solely by $\hat{\phi}$, the length of the inflaton matrices along the direction of $\mathbf{SU}(2)$. This realizes precisely the picture described earlier of the D3-branes fixed upon the surface of a 2-sphere with variable radius, now identified with the value of effective inflaton field $\hat{\phi}$.

Concordantly, the vanishing $\mathbf{\Psi}_i$ and $\mathbf{A}_\mu$ fields are referred to as *spectators*. Upon setting them to zero, the action (2.1) simplifies propitiously to

$$S = \int \mathrm{d}^4x\sqrt{-g}\left\{\frac{M_{\rm pl}^2}{2}R + \mathrm{Tr}\mathbf{J}_i^2\left(-\frac{1}{2}\partial_\mu\hat{\phi}\partial^\mu\hat{\phi} - \frac{\lambda}{2}\hat{\phi}^4 + \frac{2\kappa}{3}\hat{\phi}^3 - \frac{m^2}{2}\hat{\phi}^2\right)\right\}, \tag{2.6}$$

where $\mathrm{Tr}\mathbf{J}_i^2 = N\left(N^2-1\right)/4$, using the properties of $\mathbf{SU}(2)$. Performing a field redefinition $\phi = \sqrt{\mathrm{Tr}\mathbf{J}_i^2}\hat{\phi}$ brings the inflaton to a canonically normalized form, yielding

$$S = \int \mathrm{d}^4x\sqrt{-g}\left\{\frac{M_{\rm pl}^2}{2}R - \frac{1}{2}\partial_\mu\phi\partial^\mu\phi - V_0\left(\phi\right)\right\} \tag{2.7}$$

which is the familiar single scalar field inflationary action.

Defining effective couplings $\lambda_{\rm eff} \equiv 8\lambda/N\left(N^2-1\right)$ and $\kappa_{\rm eff} \equiv 2\kappa/\sqrt{N\left(N^2-1\right)}$ and then using the constraint that the background is a solution to the supergravity equations of motion with constant dilaton, $\lambda m^2 = 4\kappa^2/9$, the effective potential can be written, with $\mu \equiv \sqrt{2}m/\sqrt{\lambda_{\rm eff}}$, simply as

$$V_0\left(\phi\right) = \frac{\lambda_{\rm eff}}{4}\phi^4 - \frac{2\kappa_{\rm eff}}{3}\phi^3 + \frac{m^2}{2}\phi^2 = \frac{\lambda_{\rm eff}}{4}\phi^2\left(\phi-\mu\right)^2. \tag{2.8}$$

Thus, in the $\mathbf{SU}(2)$ sector, the inflationary potential of M-flation assumes the form of a symmetry-breaking potential. It has two global minima: one at $\phi = \mu$ (corresponding to a supersymmetric vacuum, when the N D3-branes blow up into a giant D5-brane wrapping a fuzzy two sphere) and one at $\phi = 0$ (corresponding to the trivial solution, when the matrices become commutative). For typical inflationary trajectories determined by this potential, all necessary parameters can be obtained by demanding certain standard requirements (namely, 60 e-foldings of inflation, together with a COBE normalization of $\delta_H \simeq 2.41 \times 10^{-5}$ and a spectral index of $n_s = 0.96$). The resultant numerical values are as follows. Further details about this analysis and the corresponding slow-roll trajectories in M-flation may be found in [23, 27]; here we just quote the results.

JCAP03(2014)020

(a) $\phi_i > \mu$. Suppose inflation starts when $\phi_i > \mu$. The aforementioned standard requirements imply

$$\phi_i \simeq 43.57 M_{\rm pl}\,, \qquad \phi_f \simeq 27.07 M_{\rm pl}\,, \qquad \mu \simeq 26 M_{\rm pl}\,, \tag{2.9}$$

and

$$\lambda_{\rm eff} \simeq 4.91 \times 10^{-14}, \qquad m \simeq 4.07 \times 10^{-6} M_{\rm pl}, \qquad \kappa_{\rm eff} \simeq 9.57 \times 10^{-13} M_{\rm pl}. \tag{2.10}$$

Taking $n_S \simeq 0.96$, the tensor/scalar ratio turns out to be 0.2 which is outside the 2σ allowed region of *Planck* in the $n_S - r$ plane. One can render this region of M-flationary phase space compatible with the data by assuming the modes start from a non-Bunch-Davies vacuum [17].

(b) $\mu/2 < \phi_i < \mu$. To fit the observational constraints we find

$$\phi_i \simeq 23.5 M_{\rm pl}\,, \qquad \phi_f \simeq 35.03 M_{\rm pl}\,, \qquad \mu \simeq 36 M_P\,, \tag{2.11}$$

and

$$\lambda_{\rm eff} \simeq 7.18 \times 10^{-14}\,, \qquad m \simeq 6.82 \times 10^{-6} M_{\rm pl}\,, \qquad \kappa_{\rm eff} \simeq 1.94 \times 10^{-12} M_{\rm pl}\,. \tag{2.12}$$

(c) $0 < \phi_i < \mu/2$. In this case we obtain

$$\phi_i \simeq 12.5 M_{\rm pl}\,, \qquad \phi_f \simeq 0.97 M_{\rm pl}\,, \qquad \mu \simeq 36 M_P\,, \tag{2.13}$$

and

$$\lambda_{\rm eff} \simeq 7.18 \times 10^{-14}\,, \qquad m \simeq 6.82 \times 10^{-6} M_{\rm pl}\,, \qquad \kappa_{\rm eff} \simeq 1.94 \times 10^{-12} M_{\rm pl}\,. \tag{2.14}$$

Due to the $\phi \to \mu - \phi$ symmetry of the background, the curvature perturbations in regions (**b**) and (**c**) turn out to have the same spectral tilt $n_S = 0.96$ and tensor-to-scalar ratio $r = 0.048$. These predictions are within the 1σ region of *Planck*-allowed parameter space. The two regions (**b**) and (**c**), however, could be distinguished by their predictions for the amplitude of isocurvature perturbations at the Hubble scale [23], as the masses of isocurvature modes do not satisfy the symmetry $\phi \to \mu - \phi$, which the classical background enjoys. As we will see, in region (**c**) the model has an embedded preheating mechanism that leads to observable gravity waves in the high frequency region.

In this way, M-flation resolves all of the problems raised earlier vis-à-vis single scalar field inflation for several reasons. First, its effective couplings can easily be made naturally small, provided N is chosen to be sufficiently large. For example, $N \approx 48\,000$ D3-branes turn out to suffice in this case for ameliorating any hierarchy problem. Second, the total amount of field displacement during M-flation has been argued [26] to be less than the UV cutoff of this model, so there is no trans-Planckian problem. Finally, this approach suggests a clear physical meaning for the inflaton, namely the radius of the two-sphere on which D3-branes live.

Despite its theoretical successes, M-flation has not been up to now extensively exploited in terms of deriving observationally testable predictions that may help set it aside from rival inflationary models. This is what we turn our attention to next, in the context of preheating.

JCAP03(2014)020

3 Preheating in M-flation

The preheating mechanism after inflation in typical models of inflation necessitates the introduction of one or more extra matter fields, or preheat fields, into which the inflaton presumably ought to decay [8, 9]. M-flation comes with this feature tacitly built-in, by way of its spectators $\mathbf{\Psi}_i$ and $\mathbf{A}_\mu$. Although, as discussed, these are assumed to be turned off classically, they can nevertheless be excited quantum mechanically. During inflation, these quantum fluctuations can cross the horizon and can become observable as isocurvature perturbations. The amplitude of the largest modes in each inflationary region was computed in [23], and shown to be generically too small to have observable effects. After inflation, however, they appear as preheat fields which can have observable effects on the GWs produced in this era.

To this end, we need to study the equations of motion and quantize their solution. We hence start with $\hat{\mathbf{\Psi}}_i$ and $\hat{\mathbf{A}}_\mu$ as perturbations in the action (2.1) — with the hats denoting "quantumness" — and deduce the resulting equations of motion. As usual in inflationary cosmic perturbation theory we assume these perturbations to be of the same order and both be much smaller than the background field values and hence keep only the first order terms in these perturbations in the equations of motion. In either case, these will take the expected form of Mathieu equations suitable for preheat fields. We discuss each case separately.

3.1 Scalar preheat fields

Setting $\hat{\mathbf{A}}_\mu = 0$ and expanding (2.1) to quadratic order in $\hat{\mathbf{\Psi}}_i$, we get [26]:

$$S^{(2)}_{\mathbf{\Psi}} = \int \mathrm{d}^4x\sqrt{-g}\left\{-\frac{1}{2}\mathrm{Tr}\left(\partial_\mu\hat{\mathbf{\Psi}}_i\partial^\mu\hat{\mathbf{\Psi}}_i\right) - \frac{1}{2}M^2_{\mathbf{\Psi}}(\phi)\,\mathrm{Tr}\left(\hat{\mathbf{\Psi}}_i^2\right)\right\}, \tag{3.1}$$

where there are two solutions for the scalar spectator masses, dubbed α-modes and β-modes respectively:

$$M^2_{\mathbf{\Psi}}(\phi) = \begin{cases} M^2_{\alpha_j}(\phi) = \dfrac{1}{2}\lambda_{\rm eff}\phi^2(j+2)(j+3) - 2\kappa_{\rm eff}\phi(j+2) + m^2, & 0 \le j \le N-2, \\ M^2_{\beta_j}(\phi) = \dfrac{1}{2}\lambda_{\rm eff}\phi^2(j-1)(j-2) + 2\kappa_{\rm eff}\phi(j-1) + m^2, & 1 \le j \le N, \end{cases} \tag{3.2}$$

with degeneracy $2j+1$ for each mode. The above ϕ-dependent masses, besides a bare mass, induce both types of $\phi^2\chi^2$ and $\phi\chi^2$ interactions for the preheat fields χ.

It can be easily shown that if inflation happens in the region (**c**), the above masses for α- and β-modes become tachyonic for an interval during the preheating era, if $j > j_{\rm min}$. For α-modes, $j_{\rm min} = 94$ and for β-modes $j_{\rm min} = 16$. For these modes, we have to alleviate the problem by including the corrections up to quartic order in $\hat{\mathbf{\Psi}}_i$.[7] We get:

$$\begin{aligned} S^{(3)}_{\mathbf{\Psi}} &= \int \mathrm{d}^4x\sqrt{-g}\left\{-\mathrm{K}_{\mathbf{\Psi}}(\phi)\,\mathrm{Tr}\left(\hat{\mathbf{\Psi}}_i^3\right)\right\}, \\ S^{(4)}_{\mathbf{\Psi}} &= \int \mathrm{d}^4x\sqrt{-g}\left\{-\Lambda_{\mathbf{\Psi}}\mathrm{Tr}\left(\hat{\mathbf{\Psi}}_i^4\right)\right\}, \end{aligned} \tag{3.3}$$

[7] The reason for inclusion of these higher order terms is to stabilize the potential for large $\hat{\mathbf{\Psi}}_i$; otherwise later simulations for the gravitational waves become unstable. We have neglected the cross-coupling that may arise from the interactions of the gauge mode and spectator mode at lower order.

JCAP03(2014)020

with

$$\mathrm{K}_{\mathbf{\Psi}}(\phi)=\begin{cases}\mathrm{K}_{\alpha_{j-2}}(\phi)=\left[\frac{\kappa_{\mathrm{eff}}}{6}-\frac{\lambda_{\mathrm{eff}}}{4}j\phi\right]\sqrt{j+1}\;\mathbb{G}_j, & 3\leq j\leq N,\\ \mathrm{K}_{\beta_{j+2}}(\phi)=\left[\frac{\kappa_{\mathrm{eff}}}{6}+\frac{\lambda_{\mathrm{eff}}}{4}\left(\frac{j+1}{2}\right)\phi\right]\sqrt{j}\;\mathbb{G}_j, & -1\leq j\leq N-2,\end{cases}\tag{3.4}$$

and

$$\Lambda_{\mathbf{\Psi}}=\begin{cases}\Lambda_{\alpha_{j-2}}=(j+1)\;\mathbb{U}_j, & 3\leq j\leq N,\\ \Lambda_{\beta_{j+2}}=j\;\mathbb{U}_j, & -1\leq j\leq N-2\,,\end{cases}\tag{3.5}$$

where

$$\begin{aligned}\mathbb{G}_j&=12\,(-1)^{N+1}\sqrt{N\left(N^2-1\right)}\sqrt{j\,(j+1)}\;\begin{pmatrix}j & j & j\\ -1 & 0 & 1\end{pmatrix}\begin{Bmatrix}j & j & j\\ \frac{N-1}{2} & \frac{N-1}{2} & \frac{N-1}{2}\end{Bmatrix},\\ \mathbb{U}_j&=\frac{\lambda_{\mathrm{eff}}}{4}N\left(N^2-1\right)\;(j+1)\sum_{c=0}^{2j}(2c+1)\begin{pmatrix}j & j & c\\ 1 & -1 & 0\end{pmatrix}^2\begin{Bmatrix}j & j & c\\ \frac{N-1}{2} & \frac{N-1}{2} & \frac{N-1}{2}\end{Bmatrix}^2,\end{aligned}\tag{3.6}$$

and $(:::)$ and $\{:::\}$ respectively denote Wigner $3j$ and $6j$ symbols [30].

We remark that the cubic couplings (3.4) are linearly dependent on the inflaton, whereas the quartic ones (3.5) are manifestly independent (i.e. they are constants for a given j). Moreover, for reasonable values of ϕ, it is plain to see that

$$\frac{\mathrm{K}_{\mathbf{\Psi}}}{M_{\mathrm{pl}}}\ll\Lambda_{\mathbf{\Psi}},\tag{3.7}$$

in virtue of the fact that the left-hand side is proportional to products of Wigner symbols, while the right-hand side is proportional to large sums of products of squares of Wigner symbols.[8] Consequently, we can treat the cubic terms as negligible. $\Lambda_{\mathbf{\Psi}}$ in general is mode dependent, however, one can show that for large j it becomes j-independent and is

$$\Lambda_{\mathbf{\Psi}}\simeq 1.0069\times 10^{11}\frac{\lambda_{\mathrm{eff}}}{4}\,.\tag{3.8}$$

One can therefore take the potential of any scalar (α or β) mode $\hat{\chi}$ to be

$$V(\phi,\hat{\chi})=V_0(\phi)+\frac{1}{2}M_{\mathbf{\Psi}}^2(\phi)\,\hat{\chi}^2+\Lambda_{\mathbf{\Psi}}\hat{\chi}^4.\tag{3.9}$$

Performing the usual Fourier decomposition

$$\hat{\chi}(t,\mathbf{x})=\int\frac{\mathrm{d}^3k}{(2\pi)^{3/2}}\;\left[\chi_k(t)\hat{a}_k\exp(-\mathrm{i}\mathbf{k}\cdot\mathbf{x})+\chi_k^*(t)\hat{a}_k^\dagger\exp(\mathrm{i}\mathbf{k}\cdot\mathbf{x})\right]$$

the corresponding equation of motion can then be written as

$$\ddot{\chi}_k+3H\dot{\chi}_k+\left(\frac{k^2}{a^2}+M_{\mathbf{\Psi}}^2(\phi)\right)\chi_k+4\Lambda_{\mathbf{\Psi}}\chi_k^3=0.\tag{3.10}$$

As we will see, this has the familiar form of a Mathieu equation in the regime where ϕ is oscillating about the vacuum (modulo the last term which, as discussed, was included to keep the potential bounded from below), and can therefore lead to parametric resonance.

[8] This claim can be easily checked by explicitly computing the couplings' numerical values for any given j.

JCAP03(2014)020

3.2 Gauge preheat fields

The story here proceeds along similar, albeit slightly simpler lines. Setting $\hat{\mathbf{\Psi}}_i = 0$ and expanding (2.1) to quadratic order in $\hat{\mathbf{A}}_\mu$ yields [26]:

$$S^{(2)}_{\mathbf{A}} = \int \mathrm{d}^4x\sqrt{-g}\left\{-\mathrm{Tr}\left(\partial_{[\mu}\hat{\mathbf{A}}_{\nu]}\partial^{[\mu}\hat{\mathbf{A}}^{\nu]}\right) - \frac{1}{2}M^2_{\mathbf{A}}(\phi)\,\mathrm{Tr}\left(\hat{\mathbf{A}}^2_\mu\right)\right\}, \tag{3.11}$$

where the mass spectrum is given by

$$M^2_{\mathbf{A}}(\phi) = \frac{1}{4}\lambda_{\rm eff}\phi^2 j(j+1), \qquad 0 \le j \le N-1. \tag{3.12}$$

The degeneracy for $j = 0$ is 2 (corresponding to massless gauge fields) while for $j \ge 1$ is $3(2j+1)$, the factor of three corresponding to the three polarizations of a four dimensional massive vector field. Unlike the scalar case, though, because (3.12) only contains a ϕ^2 term, we need not worry about the danger of acquiring tachyonic masses and the higher order corrections will always remain small compared the leading quadratic terms.[9] We can therefore safely ignore all higher-order corrections and write the equation of motion for the Fourier modes A_k of the gauge preheat fields as

$$\ddot{A}_k + H\dot{A}_k + \left(\frac{k^2}{a^2} + M^2_{\mathbf{A}}(\phi)\right)A_k = 0. \tag{3.13}$$

Despite the fact that the Hubble friction term appears with a different coefficient than in the scalar case (3.10), we still get a Mathieu equation when the inflaton ϕ oscillates around its minimum toward the end of inflation.

The next question to ask is then what the parametric resonance idiosyncratic to (3.10) and (3.13) can give us. A potentially rich and predictive product thereof is GW production.

4 Parametric resonance

4.1 SUSY-breaking vacuum

If the initial condition is such that inflation happens in regions (**a**) or (**b**), the inflaton will finally end up oscillating around the SUSY-breaking vacuum, $\phi = \mu$. It might be thought the inflaton oscillations around the vacuum, $\phi = \mu$, and its couplings to different preheat fields can create parametric resonance. However, it can be shown that the rest masses of α and β modes in this region are so large that non-adiabatic particle production is suppressed. To be specific, let us focus on α-modes and β-modes. A similar analysis and argument could be repeated for the gauge modes as well.

The mass functions for the α and β modes can be unified in the following form

$$M^2_{\mathbf{\Psi}}(\phi) = \frac{1}{2}\lambda_{\rm eff}\omega(\omega-1)\phi^2 + 2\kappa_{\rm eff}\phi\omega + m^2, \tag{4.1}$$

where

$$\omega = \begin{cases} -(j+2) & 1 \le j \le N-2, \\ (j-1) & 1 \le j \le N. \end{cases} \tag{4.2}$$

[9] Note that massless gauge field states do not couple to the background effective inflaton (as the effective inflaton is a real field and massless gauge fields are in the center $\mathbf{U}(1)$ of the $\mathbf{U}(N)$ gauge symmetry. The $\mathbf{U}(N)$ gauge symmetry is spontaneously broken to $\mathbf{U}(1)$ by the background field configuration.

JCAP03(2014)020

Expanding the interaction term around the SUSY-breaking vacuum $\phi = \mu$ and introducing the variable $\varphi \equiv \phi - \mu$, the interaction term between the inflaton and spectators looks like[10]

$$V_{\rm int} = \frac{1}{2} g_4^2 \varphi^2 \hat{\chi}^2 + \frac{1}{2} g_3 \varphi \hat{\chi}^2 + \frac{1}{2} m_{\hat{\chi}}^2 \hat{\chi}^2, \tag{4.3}$$

where

$$\begin{aligned} g_4^2 &= \frac{\lambda_{\rm eff}\left(\omega^2 - \omega\right)}{2}, \\ g_3 &= \frac{1}{2}\lambda_{\rm eff}\mu\left(2\omega^2 + \omega\right), \\ m_{\hat{\chi}}^2 &= \frac{\lambda_{\rm eff}\mu^2}{2}(\omega+1)^2 = m^2(1+\omega)^2, \end{aligned} \tag{4.4}$$

and φ varies between zero and $\Phi = \mu - \phi_f \simeq 1 M_{\rm pl}$. Despite the existence of interactions like $\varphi\hat{\chi}^2$, since the rest masses of all the $\hat{\chi}$ fields are larger or equal to the mass of the inflaton, perturbative decay of the inflaton to none of the $\hat{\chi}$ fields is possible.[11]

Around the SUSY-breaking vacuum, the inflaton potential to a large extent resembles $\frac{1}{2}m^2\varphi^2$. Therefore, the inflaton has an oscillatory behavior $\varphi(t) \approx \Phi \sin(mt)$ [8, 9] around the SUSY-breaking vacuum. It can be shown that the contribution of the $g_4^2\phi^2\hat{\chi}^2$ interaction is subdominant with respect to the $g_3\phi\hat{\chi}^2$ for all ω's. The ratio of two interactions is

$$R \equiv \frac{g_4^2\varphi(t)^2\hat{\chi}^2}{g_3\varphi(t)\hat{\chi}^2} \approx \frac{\omega - 1}{2\omega + 1}\frac{\Phi}{\mu}\sin(mt). \tag{4.5}$$

For all values of $\omega > 0$ this ratio is less than one,[12] since the ratio $\Phi/\mu \lesssim 0.04$ in both the (**a**) and (**b**) regions. Thus we will drop this quartic interaction term in comparison with the cubic one in the rest of the analysis.

Let us analyze (3.10) in a non-expanding background where $a = 1$. Dropping the contribution of the quartic interaction, for an oscillating inflaton the approximated equation takes the form

$$\ddot{\hat{\chi}}_k + \left(k^2 + m_{\hat{\chi}}^2 + \frac{\lambda_{\rm eff}\mu\Phi}{2}\omega(2\omega+1)\sin(mt)\right)\hat{\chi}_k = 0. \tag{4.6}$$

Introducing the new variable $z \equiv \frac{mt}{2} + \frac{\pi}{4}$ and $' \equiv \frac{d}{dz}$, the equation takes the form of a Mathieu equation [32]

$$\hat{\chi}'' + (A_k - 2q\cos(2z))\hat{\chi} = 0, \tag{4.7}$$

where

$$A_k \equiv \frac{4\left(k^2 + m^2\right)}{m^2}, \tag{4.8}$$

$$q \equiv \frac{\lambda_{\rm eff}\mu\Phi\omega(2\omega+1)}{m^2} = \frac{2\Phi}{\mu}\omega(2\omega+1). \tag{4.9}$$

It is known [33] that equation (4.7) has solutions with an exponential instability $\hat{\chi} \propto \exp\left(\mu_k^{(n)} z\right)$ that represent a burst of particle production. The solutions have resonance

[10] In the rest of the analysis we will drop the quartic $\Lambda_\Psi\hat{\chi}^4$ term. As we will see in the next subsection presence of this term weakens the particle production and thus strengthens our results.

[11] For the same reason the tachyonic resonance of [31] does not occur in our case.

[12] $\omega = 0$ (the $j = 1$ β mode) does not have any interaction with the inflaton.

JCAP03(2014)020

bands with the width $\Delta k^{(l)} \simeq q^l$. If $q \ll 1$, what is known as narrow resonance band, the resonance occurs in bands near $A_k \simeq l^2$, where l is a nonzero integer. Hence the widest band is the first instability band. Imposing the condition $q < 1$ for the inflationary region (**a**) where $\mu \simeq 26\ M_{\rm pl}$, only $0 \leq \omega \leq 2$ ($1 \leq j \leq 3$ β modes) lead to narrow resonance. In the region (**b**), where $\mu < 36$, besides the aforementioned modes, $\omega = -3$ ($j = 1$ α mode) can also lead to narrow resonance. The factor μ_k, the Floquet index, for the first instability band is given by [8, 9]

$$\mu_k = \sqrt{\left(\frac{q}{2}\right)^2 - \left(\frac{2k}{m} - 1\right)^2}, \tag{4.10}$$

where the resonance happens for the narrow momentum k range $1 - \frac{q}{2} \leq \frac{2k}{m} \leq 1 + \frac{q}{2}$. It obtains its maximum at $\mu_k = q/2$ at $k = m/2$.

In an expanding background the redshift of momentum k from the resonance band can prevent the resonance. As pointed out in [8, 9], the condition for the first band to be effective during expansion is

$$q^2 m \gtrsim H. \tag{4.11}$$

The inequality is not satisfied for the modes that can undergo parametric resonance in flat space-time. This is because during preheating $H \simeq 0.1m$ [8, 9] and $\Phi^2/\mu^2 \lesssim 1.5 \times 10^{-3}$. Thus narrow parametric resonance for these modes cannot lead to preheating.

For larger values of ω, the resonance is broad. However, one can show that the large rest mass of these modes, $m_{\hat{\chi}} = m(\omega + 1)$, and the smallness of the amplitude of oscillations with respect to the supersymmetry-breaking vacuum μ, shuts off the particle production. To see this, let us note that the time-dependent frequency in the equation of motion for $\hat{\chi}$ in an expanding background is given by

$$\Omega = \sqrt{\frac{k^2}{a^2} + m_{\hat{\chi}}^2 + \frac{\lambda_{\rm eff}\mu\Phi}{2}\omega(2\omega + 1)\sin(mt)}. \tag{4.12}$$

The condition for the adiabaticity violation is that

$$\left|\frac{\dot{\Omega}}{\Omega^2}\right| \simeq \frac{1}{2}\frac{\omega(2\omega+1)\cos(mt)}{m((\omega+1)^2 - \omega(2\omega+1)\frac{\Phi}{\mu}\sin(mt))^{3/2}}\frac{\Phi}{\mu} \gtrsim 1, \tag{4.13}$$

a condition that cannot be satisfied for large values of ω due to the smallness of Φ/μ. Similar arguments can be given for the gauge spectator modes.

Recapitulating our results, it is not possible to reheat M-flation around the SUSY-breaking minimum via any of the α, β or gauge spectators modes. The supersymmetric model is equipped with fermionic spectators that might contribute to this process. Nonetheless, due to Pauli exclusion, resonances cannot happen for fermionic modes and considering them will not change the above result.

4.2 Supersymmetric vacuum

Unlike the supersymmetry breaking vacuum, parametric resonance around $\phi = 0$ (supersymmetric vacuum) can be quite effective through the spectator modes. We first focus on the scalar preheat fields. The equation of motion for the perturbations $\mathbf{\Psi}_i$ can be decomposed into the equation of motion for the α and β spectator modes which in Fourier space takes the form

$$\ddot{\hat{\chi}}_k + 3H\dot{\hat{\chi}}_k + \left(\frac{k^2}{a^2} + \frac{\lambda_{\rm eff}}{2}\phi^2\left(\omega^2 - \omega\right) + \frac{3}{2}\mu\lambda\omega\phi + m^2\right)\hat{\chi}_k + 4\Lambda_{\mathbf{\Psi}}\hat{\chi}_k^3 = 0. \tag{4.14}$$

JCAP03(2014)020

The bare masses of the spectator modes are equal to the inflaton mass m^2 and in principle for large values of ω, the adiabatic condition may be broken violently. However, as we will see, self-interactions of the $\hat{\chi}$ particles, incorporated in the last term of the equation of motion, slows down the parametric resonance.

In terms of the dimensionless time variable $\tilde{z}$, defined as

$$\tilde{z} \equiv mt, \tag{4.15}$$

the equations of motion for the inflaton and the background are

$$\phi'' + 3\mathcal{H}\phi' + \left(\frac{2\phi^3}{\mu^2} - \frac{3\phi^2}{\mu} + \phi\right) = 0, \tag{4.16}$$

$$\mathcal{H}^2 = \frac{1}{3M_{\rm pl}^2}\left[\frac{1}{2}\phi'^2 + \frac{1}{2}\phi^2\left(\frac{\phi}{\mu} - 1\right)^2\right], \tag{4.17}$$

where

$$\mathcal{H} \equiv \frac{a'}{a}. \tag{4.18}$$

The equation of motion for the Fourier mode, $\mathcal{X}_k \equiv a^{3/2}\hat{\chi}_k$, is

$$\mathcal{X}_k'' + {\Omega_k}^2\mathcal{X}_k + \frac{4\Lambda_{\Psi}}{a^3m^2}\mathcal{X}_k^3 = 0, \tag{4.19}$$

where

$${\Omega_k}^2 \equiv \frac{k^2}{m^2a^2} + \frac{\phi^2}{\mu^2}\left(\omega^2 - \omega\right) + \frac{3\phi}{\mu}\omega + 1 - \frac{3}{4}\mathcal{H}^2 - \frac{3}{2}\frac{a''}{a}. \tag{4.20}$$

Eq. (4.19) can be solved imposing the Bunch-Davies vacuum on the mode $\mathcal{X}_k$

$$\mathcal{X}_k \to \frac{e^{-i\frac{\Omega_k t'}{m}}}{\sqrt{2\Omega_k}} \tag{4.21}$$

at the beginning of preheating. The number density for the produced particles is [8, 9]

$$n_k^{\mathcal{X}} = \frac{\Omega_k}{2}\left(m^2\frac{|\mathcal{X}_k'|^2}{\Omega_k^2} + |\mathcal{X}_k|^2\right) - \frac{1}{2}. \tag{4.22}$$

To demonstrate the contribution of the cubic term to the comoving number density, we have numerically solved the equations for perturbation in the presence and absence of the cubic contribution to the equations of motion (4.19) for $k = 0$ for the largest j β-mode. As can be seen in the L.H.S. graph of figure 1, in the absence of the cubic term, the number density of the produced particles exhibits stochastic resonance behavior [8, 9], i.e. it typically increases at some specific moments but it may decrease as well. In between these instants, the number density remains approximately constant (sharp oscillations on the plateaus are only numerical artifacts). The interval between the kicks in n_k is roughly about π, which is the small interval in which the mode becomes massless and tachyonic. However, once the cubic term (from the quartic self-coupling term) is added to the equation of motion (4.19), n_k ceases to exhibit resonance behaviour initially, its value being highly suppressed. This continues until the cubic term in the equation of motion of the scalar spectator redshifts and the mode revert to resonance behaviour.

JCAP03(2014)020

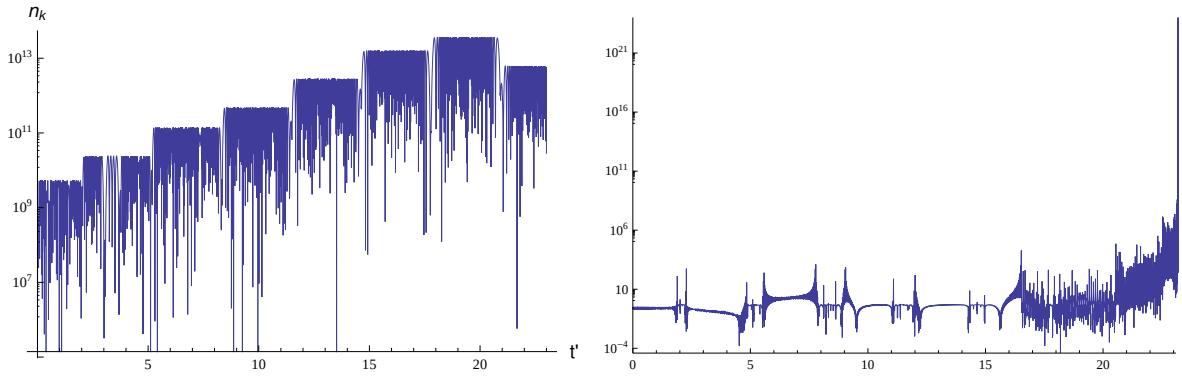

Figure 1. Left graph shows how the comoving number density of the $\hat{\chi}$ particles, n_k^{χ} evolves as a function of $\tilde{z}$ for $k = 0$, in the absence of the quartic self-coupling term, which explicitly exhibits the stochastic resonance behavior. The right figure shows the same when the quartic coupling term is added to the Lagrangian of the $\hat{\chi}$ field. As can be seen, the self-coupling term slows down the resonance.

For the gauge mode the equation of motion is given by (3.13). Introducing the new variable

$$\mathcal{A}_k = a^{1/2} A_k, \tag{4.23}$$

the equation takes the following form

$$\mathcal{A}_k'' + \tilde{\Omega}_k^2 \mathcal{A}_k = 0, \tag{4.24}$$

where

$$\tilde{\Omega}_k^2 \equiv \frac{k^2}{m^2 a^2} + \frac{\phi^2}{2\mu^2}\left(j^2 + j\right) + \frac{1}{4}\mathcal{H}^2 + 1 - \frac{a''}{2a}. \tag{4.25}$$

Again (4.24) can be solved numerically imposing the Bunch-Davies vacuum in infinite past for the $\mathcal{A}_k$.

We have numerically solved (4.24) for $k = 0$. As it can be seen in figure 2 the gauge mode number density of produced particles, which is given by [8, 9]

$$n_k^{\mathcal{A}} = \frac{1}{a^2}\left[\frac{\tilde{\Omega}_k}{2}\left(m^2\frac{|\mathcal{A}_k'|^2}{\tilde{\Omega}_k^2} + |\mathcal{A}_k|^2\right) - \frac{1}{2}\right], \tag{4.26}$$

also demonstrates stochastic resonance behaviour. Note that the $1/a^2$ factor in $n_k^{\mathcal{A}}$ will in principle cause the gauge mode particles to dilute. The comoving number density of the particles overall increases more slowly due to the expansion of the universe. The production of gauge modes happens in brane-antibrane inflation too [14].

5 Gravity Waves from preheating around the SUSY vacuum

Effective preheating can lead to explosive particle creation and, consequently, the production of stochastic Gravitational Waves (GWs) [15, 16]. The latter arise from the tensor modes h_{ij} of perturbations to the FRW metric, and are linked to the former via the perturbed Einstein equations,

$$\ddot{h}_{ij} + 3H\dot{h}_{ij} - \left[\frac{\nabla^2}{a} + 2\left(H^2 + 2\frac{\ddot{a}}{a}\right)\right] h_{ij} = \frac{16\pi G}{a^2}\delta S_{ij}^{\mathrm{TT}}, \tag{5.1}$$

JCAP03(2014)020

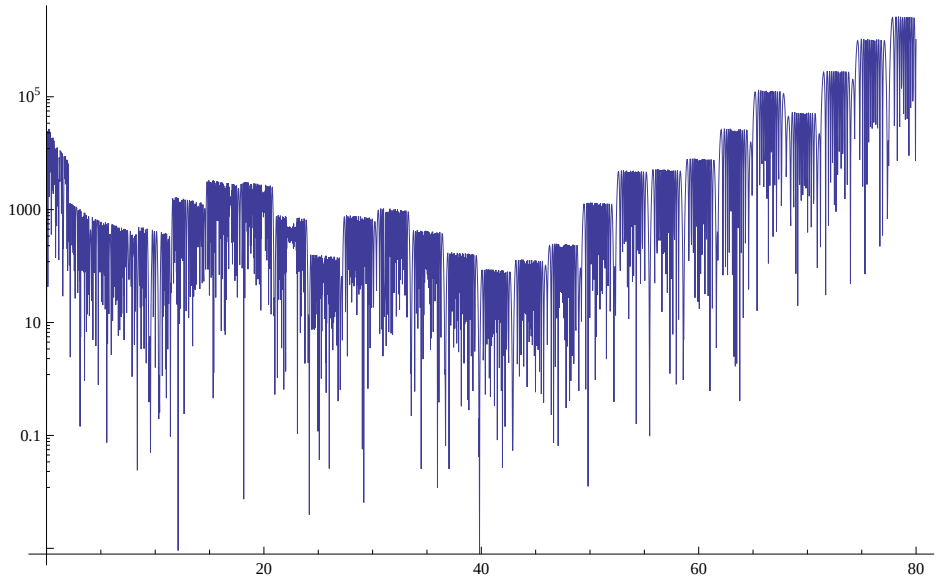

Figure 2. $n_k^{\mathcal{A}}$ vs. $\tilde{z}$. Despite the decrease in the number density of the produced gauge particle, the number density exhibits a stochastic resonance behavior.

where $\delta S_{ij}^{\rm TT}$ is the transverse-traceless part of the stress tensor perturbation $\delta S_{ij} = \delta T_{ij} - \frac{1}{3}\delta_{ij}\delta T_k{}^k$ which depends by construction on the number density and energy of the preheat fields. This stress-tensor perturbations are receiving contribution from the particles produced during the preheating era discussed in the previous section, which in turn source the gravity waves through (5.1).

Recalling that the Landau-Lifshitz pseudotensor [34] associated with gravitational radiation is $T_{\mu\nu} = \langle h_{ij,\mu} h^{ij}{}_{,\nu} \rangle / 32\pi G$, we can write the ratio between the spectral energy density thereof and the present-day total energy density as

$$\Omega_{\rm gw}(f) = \frac{1}{\rho_c}\frac{\mathrm{d}}{\mathrm{d}\ln f} T_{00} = \frac{1}{\rho_c}\frac{\mathrm{d}}{\mathrm{d}\ln f}\sum_{i,j}\frac{1}{32\pi G}\left\langle h_{ij,0}^2 \right\rangle, \tag{5.2}$$

where f denotes the GW frequency. Using this, it is in principle possible to compute the power spectrum, $\Omega_{\rm gw}h^2$.

Of course, the dynamics involved are highly nonlinear and far too complicated to render this task analytically tractable; instead, we resort to numerics. Thus, to determine the power spectrum of GW generated during preheating after inflation by the various scalar and gauge modes described in the previous section, we employ the lattice simulator HLattice 2.0 [28].

HLattice is generically designed to solve equations of motion via a numerical scheme known as *symplectic integration*, which is typically very stable and often used for long-term many-body simulations in astronomy and particle physics. The basic idea of how it works is as follows (for a detailed overview, the reader is referred to [28]).Spatial coordinates are discretized on a three-dimensional lattice — in our cases, with 64 grid points along each edge — and time evolution is achieved by considering the Hamiltonian $\mathcal{H}$ of the system which, in lieu of a spatial integral, can be written as a sum over all of the lattice points. Then, any arbitrary function F evolves via

$$\frac{\mathrm{d}F}{\mathrm{d}t} = \{F, \mathcal{H}\} \equiv \hat{\mathbf{H}}F,$$

JCAP03(2014)020

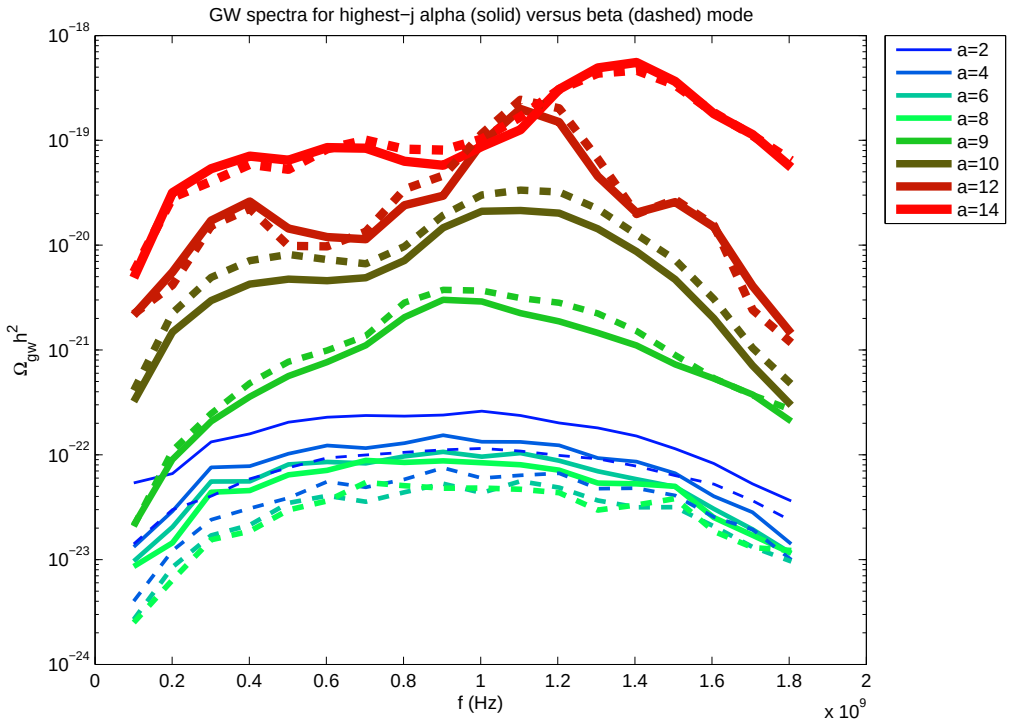

Figure 3. GW amplitude as a function of frequency due to the highest-j scalar modes, both α (solid) and β (dashed), for a range of scale factors from $a = 1$ (beginning of preheating) to $a = 14$.

where $\{\cdot, \cdot\}$ is the Poisson bracket and $\hat{\mathbf{H}}$ is the corresponding functional operator. The solution is thus

$$F\left(t + \mathrm{d}t\right) = \mathrm{e}^{\hat{\mathbf{H}}\mathrm{d}t} F(t).$$

An n-th order symplectic integrator is constructed by factorizing $\exp\left(\hat{\mathbf{H}}\mathrm{d}t\right)$ into a product of exponentials of the constituent (kinetic and potential) terms of the Hamiltonian up to $\mathcal{O}\left(\mathrm{d}t^{n+1}\right)$. While HLattice 2.0 is in principle able to implement this up to sixth order (using a fourth order Runge-Kutta subintegrator, with a time step much smaller than $\mathrm{d}t$, to solve the resulting equations of motion), we simply used its second order symplectic integrator in obtaining all of the results that follow, for the sake of keeping computational times manageable.

5.1 GW from scalar modes

The power spectra of GW due to the most massive — i.e. highest j — scalar modes (both α and β) are shown in figure 3. The scale factor is normalized to $a = 1$ at the end of inflation/beginning of preheating, and we carry out the computation up to $a = 14$, when the spectrum becomes UV dominated. Indeed, after preheating, field energies typically cascade towards the UV,[13] and in HLattice this renders all further (higher a) computations non-physical because of the finite resolution of the simulator as well as its lacking treatment of quantum effects at very high wavenumbers [36]. To illustrate this, we plot the kinetic energy

[13]Note that all simulations start out (small a) "UV dominated" and have larger energies at larger wave lengths. However, they do not remain so. However there is a later time (larger a) which become UV dominated again.

JCAP03(2014)020

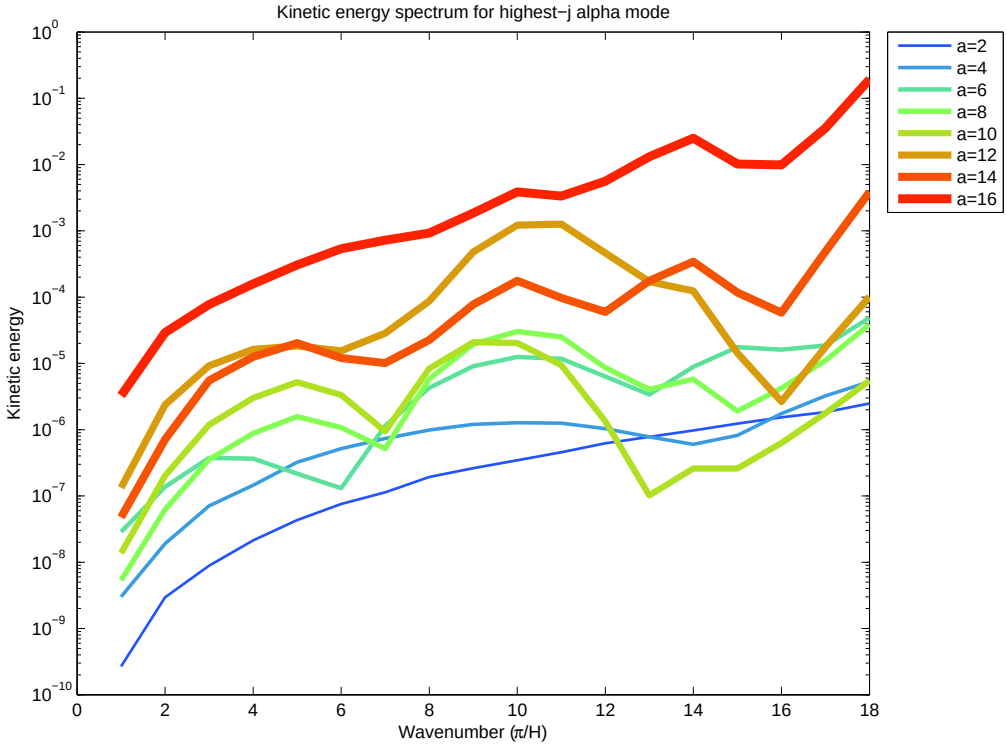

Figure 4. Kinetic spectrum of the highest j α mode (in units of the background energy density) vs. the wavenumber in units of $\frac{\pi}{H}$. That is, the plot shows, $\frac{k^3}{4\pi^2}\left[\frac{k^2}{a^2}|\chi_k|^2\right]/(\rho_{\rm background})$ vs $\frac{kH}{\pi}$.

spectrum of the highest j α mode in figure 4 and observe that it starts to be dominated at the UV end for $a \geq 14$.

We remark that, as is seen in figure 3, the two α and β types of scalar preheat fields produce very similar GW spectra, as may well be expected from inspecting their masses (3.2) and quartic couplings (3.5): for large j, both α and β type preheat fields have an approximate mass of

$$M_{\Psi}^2(\phi) \approx \frac{1}{2}\lambda_{\rm eff}\phi^2 j^2, \tag{5.3}$$

and quartic coupling of

$$\Lambda_{\Psi} \approx j^2\left[\frac{\lambda_{\rm eff}}{4}N\left(N^2-1\right)\right]\sum_{c=0}^{2j}(2c+1)\begin{pmatrix} j & j & c \\ 1 & -1 & 0\end{pmatrix}^2\begin{Bmatrix} j & j & c \\ \frac{N-1}{2} & \frac{N-1}{2} & \frac{N-1}{2}\end{Bmatrix}^2. \tag{5.4}$$

In producing these graphs we have assumed that $N = 48000$. We have also taken the largest j α and β modes individually, i.e. $j = 48000$ single β and α mode.

5.2 GW from gauge modes

The GW power spectrum due to the most massive gauge mode, up to $a = 7$, before the UV domination kicks in, is shown in figure 5. Again we have focused on the largest j gauge mode, $j = 47999$. As in the scalar mode case, the amplitude grows with increasing scale factor under the clear effect of parametric resonance. However the growth is much faster: amplitudes become as large as 10^{-11} by $a = 7$, at which point the computations become

JCAP03(2014)020

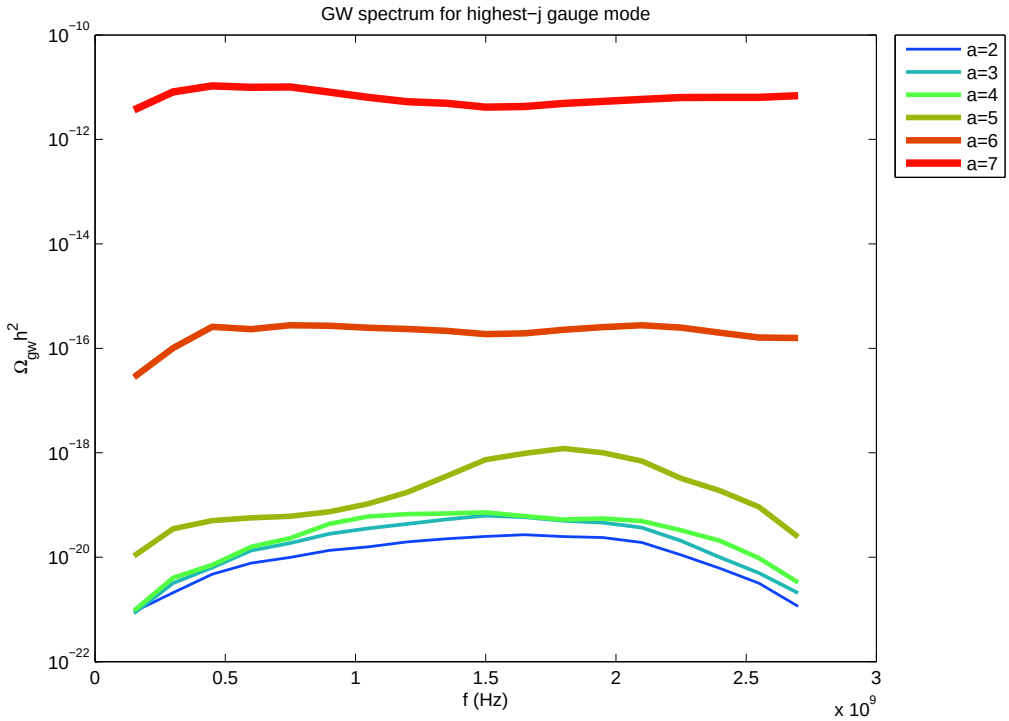

Figure 5. GW amplitude as a function of frequency due to the highest-j gauge mode, for a range of scale factors from $a = 1$ (beginning of preheating) to $a = 7$.

UV dominated. The difference between gauge and scalar modes is essentially coming from the difference in their corresponding equations, and in particular the difference between Ω_k (4.20) and $\tilde{\Omega}_k$ (4.25). The delay in the enhancement of GW spectrum from scalar modes could be traced back to the fact that the presence of cubic coupling term in their equations of motion generically slows down the resonance. To compare the contributions to the total GW spectrum from the scalar and gauge modes, they are plotted together in figure 6. The spectrum from a single gauge mode is also flatter in comparison with its scalar counterpart, but still a double hump feature of the gravity profile from preheating can be distinguished.

Thus, we see that the spectrum of GW produced by preheating following M-flation is dominated by the gauge preheat fields, which give rise to GW amplitudes more than 10 orders of magnitude greater (at a=7) than those due to (either type of) their scalar counterpart.

5.3 GW from several gauge modes

As noted above the spectrum of GWs from the gauge modes dominate the scalar modes by 10 orders of magnitude. This suggests that if all three modes are run together as the preheat fields, the gauge modes are more effective in the production of GWs. However this was done for a single scalar or gauge mode and at large j there are $\sim 2j$ (for scalars) and $\sim 6j$ (for vectors) such modes for a given j. In principle one should consider the effects of all the degenerate modes. It may seem from (5.1) and (5.2) that the GW power spectrum should grow like $j^2 \sim N^2$. However, given the highly nonlinear character of these equations this expectation can only hold for a very short time in the very low frequency region where the nonlinear effects are negligible. The larger the degeneracy, the earlier the UV domination, and hence modes have a shorter growth time. This is compatible with the

JCAP03(2014)020

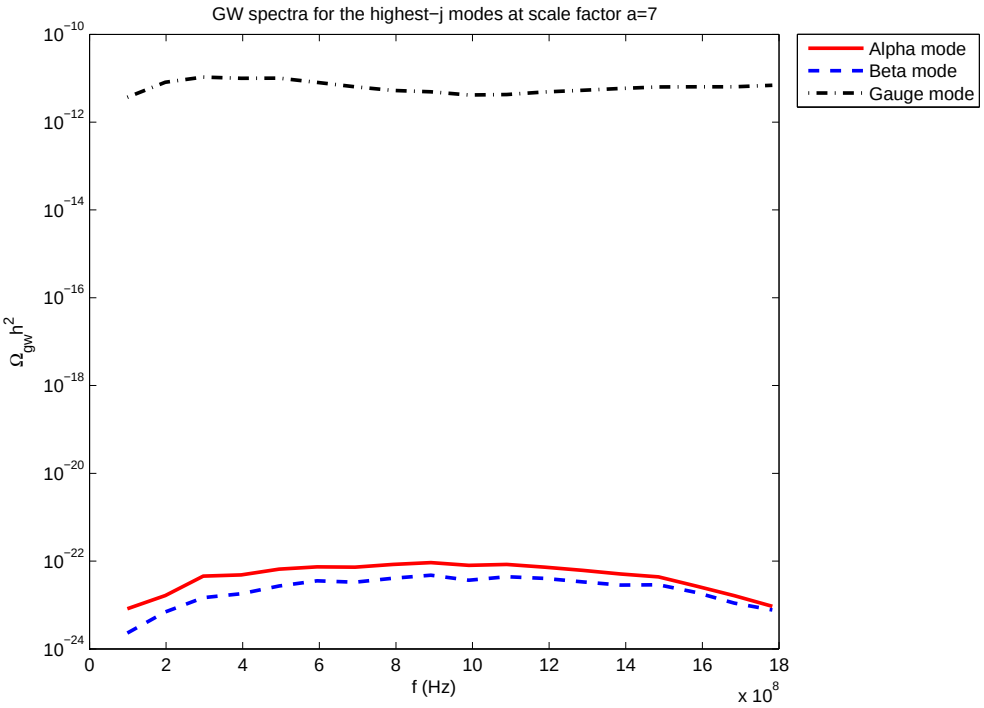

Figure 6. GW amplitude as a function of frequency due to the highest-j modes, both scalar (α in solid and β in dashed) and gauge (dashed-dotted), at scale factor $a = 7$.

analysis of [35]. However one should note that in the study of [35] the preheat modes are scalar fields, whereas the ones in our simulations are gauge modes, i.e. they appear with the friction term proportional to H, instead of $3H$ in the equations of motion.

Given the fact that for large j gauge modes have a $6j$ degeneracy, to check the effects of degeneracies in our setup we should simulate the effect of $3 \times 95999 = 287997$ gauge mode as preheat fields. This number is quite huge and cannot be handled without substantial computational resources. To get an idea of the effects of degeneracy, we tried three and six gauge modes.[14]

To explore the degeneracy effects more clearly we have shown the spectrum of GWs from one, three and six largest j gauge modes in the same plot, figure 7. Although these data are not enough for making precise deductions, they still exhibit the following features:

- *Time dependence.* At the beginning of preheating, low a up to $a = 3$, the amplitude of the GW spectrum resulting from the three and six gauge preheat modes, is larger than that of the single mode. As pointed out in [35], this is the stage the inflaton is coherently oscillating around its minimum and non-linear effects have not yet kicked in. However, as the inhomogeneities of the inflaton grow, gravitational radiation is counteracted by the backreaction and the model with multiple preheat fields stops being efficient; nonlinear effects suppress the degeneracy effects and we see no large degeneracy effect. Moreover, UV domination happens earlier (at lower a) for larger degeneracy such that the amplitude of GWs is almost degeneracy independent.

[14] We should note that the simulation of a single mode with highest j-number up to the onset of UV domination took a week to perform on the Sharcnet cluster of the University of Waterloo. In comparison with previous studies on gravitational wave production from preheating, this is due to the large value of coupling of the inflaton to the preheat field which is of order $\lambda_{\rm eff} N^2 \sim 1.6 \times 10^{-4}$.

JCAP03(2014)020

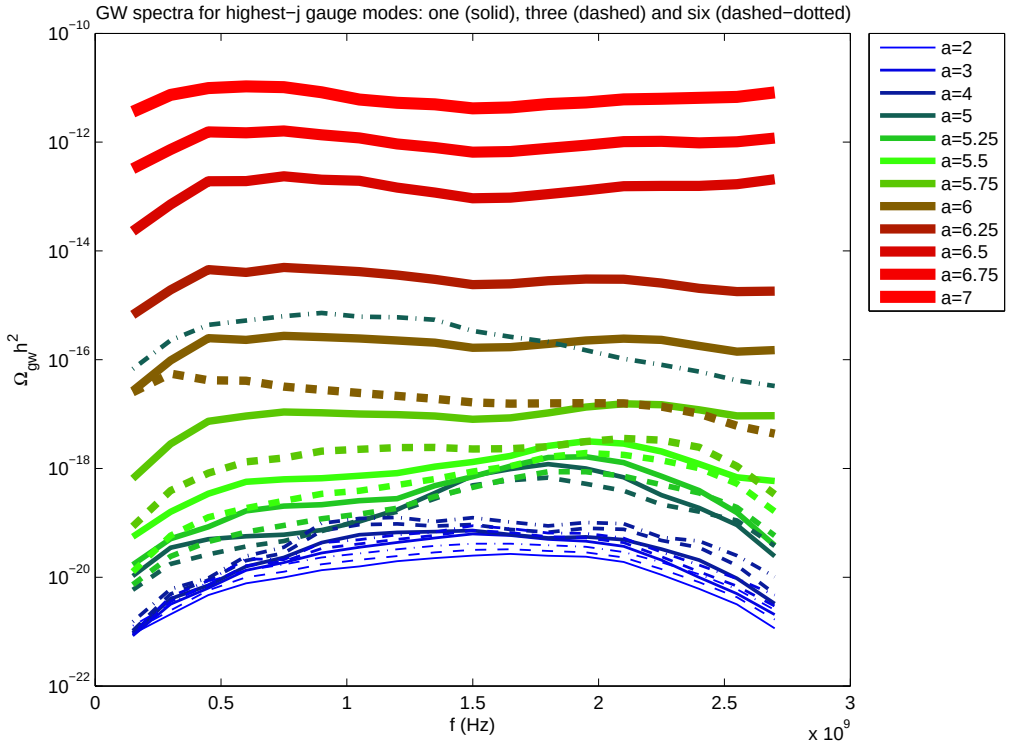

Figure 7. Gravitational wave profile from one, three and six highest j gauge modes until their corresponding onset of UV domination. The larger the numbers of preheat fields, the earlier the the onset of UV domination.The spectrum generated from three and six gauge modes become steeper at the high frequency tail in comparison with that of the single mode.

- *Frequency dependence.* Besides the amplitude of the produced GWs, frequency is the distinctive observational feature in our model. Our current data with six gauge preheat modes already shows that the GWs of our model are in the $1-3$ GHz band and they are almost flat with amplitudes around 10^{-16}. Revealing the exact amplitude of the GW spectrum and its finer features in this range needs an analysis with a larger number of modes.

6 Concluding remarks

In this work we extended the analysis of [21, 23, 27] on the M-flation model. As discussed, M-flation helps with the resolution of many of the principal theoretical difficulties endemic to standard scalar field inflationary models. Moreover, M-flation is also able to furnish concrete observational predictions courtesy of its built-in preheating mechanism around the $\phi = 0$ vacuum. In search for possible, beyond CMB, observational signatures of M-flation we have analyzed the power spectra of gravitational waves produced in this model due to the different types of its preheat fields. We have found that the gauge preheat fields contribute overwhelmingly to this process as compared to their scalar counterparts, producing a large amplitude spectrum in the few GHz band with an amplitude of order 10^{-16}. It is hoped that such a spectrum could be observed by ultra-high frequency GW detectors that may be able to probe the GHz band, such as the Birmingham HFGW resonant antenna [37–39] or the one

JCAP03(2014)020

at Chongqin University [40, 41]. The Birmingham detector works based on the detection of the rotation of the polarization vector of an electromagnetic wave induced by the interaction between a gravitational wave and the polarization vector of the electromagnetic wave. The sensitive frequency range is at 10^8 HZ. The Chongqing detector exploits the electromagnetic interaction of a Gaussian beam propagating through a static magnetic field. These detectors work based on different principles from the phase measurement with the laser interferometry developed in the ground-based large-scale interferometers around few hundred Hz.

One should note that the GW spectrum we discussed in this paper is in the high frequency range, and is in addition to the spectrum of gravity waves (tensor modes) that the model produces at the CMB scales, with the tensor-to-scalar ratio $r \simeq 0.048$ [23]. In addition the lightest spectator mode in this inflationary region will create a substantial amplitude of isocurvature perturbations with amplitude $P_{\mathcal{S}}/P_{\mathcal{R}} \simeq 5 \times 10^{-3}$ which has a degeneracy of three [23].[15] These features could be used to distinguish M-flation in this region from other inflationary models.

Acknowledgments

We are greatly indebted to Z. Huang for his extensive help and advice in our implementation of the HLattice 2.0 code used here. This work was supported in part by the Natural Sciences and Engineering Research Council of Canada. M.O. acknowledges additional support from the University of Waterloo Department of Physics and Faculty of Mathematics. A.A. is supported by the Lancaster-Manchester-Sheffield Consortium for Fundamental Physics under STFC grant ST/J000418/. A.A. also acknowledges the hospitality of Uppsala Institute for Theoretical Physics during the completion of this work.

References

[1] Planck collaboration, P.A.R. Ade et al., *Planck 2013 results. XXII. Constraints on inflation*, arXiv:1303.5082 [INSPIRE].

[2] V. Mukhanov, *Physical Foundations of Cosmology*, Cambridge University Press, (2005).

[3] S. Weinberg, *Cosmology*, Oxford University Press, Oxford, U.K. (2008).

[4] D.H. Lyth and A.R. Liddle, *The primordial density perturbation: Cosmology, inflation and the origin of structure*, Cambridge University Press, Cambridge, U.K. (2009).

[5] A. Maleknejad, M.M. Sheikh-Jabbari and J. Soda, *Gauge Fields and Inflation*, *Phys. Rept.* **528** (2013) 161 [arXiv:1212.2921] [INSPIRE].

[6] C. Armendariz-Picon, T. Damour and V.F. Mukhanov, *k-inflation*, *Phys. Lett.* **B 458** (1999) 209 [hep-th/9904075] [INSPIRE].

[7] L. Kofman, A.D. Linde and A.A. Starobinsky, *Reheating after inflation*, *Phys. Rev. Lett.* **73** (1994) 3195 [hep-th/9405187] [INSPIRE].

[8] L. Kofman, A.D. Linde and A.A. Starobinsky, *Towards the theory of reheating after inflation*, *Phys. Rev.* **D 56** (1997) 3258 [hep-ph/9704452] [INSPIRE].

[9] P.B. Greene, L. Kofman, A.D. Linde and A.A. Starobinsky, *Structure of resonance in preheating after inflation*, *Phys. Rev.* **D 56** (1997) 6175 [hep-ph/9705347] [INSPIRE].

[10] B. Bassett, *The preheating-gravitational wave correspondence: 1.*, *Phys. Rev.* **D 56** (1997) 3439 [hep-ph/9704399] [INSPIRE].

[15] We note that the *Planck* bound is $P_{\mathcal{S}}/P_{\mathcal{R}} < 3.6 \times 10^{-2}$ [1].

JCAP03(2014)020

[11] A.B. Henriques and R.G. Moorhouse, *Cosmic microwave background and parametric resonance in reheating*, *Phys. Rev.* **D 65** (2002) 103524 [hep-ph/0109218] [INSPIRE].

[12] S. Tsujikawa and B.A. Bassett, *When can preheating affect the CMB?*, *Phys. Lett.* **B 536** (2002) 9 [astro-ph/0204031] [INSPIRE].

[13] S.-Y. Zhou, E.J. Copeland, R. Easther, H. Finkel, Z.-G. Mou and P.M. Saffin, *Gravitational Waves from Oscillon Preheating*, *JHEP* **10** (2013) 026 [arXiv:1304.6094] [INSPIRE].

[14] A. Mazumdar and H. Stoica, *Exciting gauge field and gravitons in a brane-anti-brane annihilation*, *Phys. Rev. Lett.* **102** (2009) 091601 [arXiv:0807.2570] [INSPIRE].

[15] S.Y. Khlebnikov and I.I. Tkachev, *Relic gravitational waves produced after preheating*, *Phys. Rev.* **D 56** (1997) 653 [hep-ph/9701423] [INSPIRE].

[16] R. Easther and E.A. Lim, *Stochastic gravitational wave production after inflation*, *JCAP* **04** (2006) 010 [astro-ph/0601617] [INSPIRE].

[17] A. Ashoorioon, K. Dimopoulos, M.M. Sheikh-Jabbari and G. Shiu, *Reconciliation of High Energy Scale Models of Inflation with Planck*, *JCAP* **02** (2014) 025 [arXiv:1306.4914] [INSPIRE].

[18] A. Ashoorioon, P.S.B. Dev and A. Mazumdar, *Implications of purely classical gravity for inflationary tensor modes*, arXiv:1211.4678 [INSPIRE].

[19] J. Martin, C. Ringeval, R. Trotta and V. Vennin, *The Best Inflationary Models After Planck*, arXiv:1312.3529 [INSPIRE].

[20] R.H. Brandenberger, *Introduction to Early Universe Cosmology*, PoS(ICFI 2010)001 [arXiv:1103.2271] [INSPIRE].

[21] A. Ashoorioon, U. Danielsson and M.M. Sheikh-Jabbari, *1/N Resolution to Inflationary η-Problem*, *Phys. Lett.* **B 713** (2012) 353 [arXiv:1112.2272] [INSPIRE].

[22] D.H. Lyth, *What would we learn by detecting a gravitational wave signal in the cosmic microwave background anisotropy?*, *Phys. Rev. Lett.* **78** (1997) 1861 [hep-ph/9606387] [INSPIRE].

[23] A. Ashoorioon, H. Firouzjahi and M.M. Sheikh-Jabbari, *M-flation: Inflation From Matrix Valued Scalar Fields*, *JCAP* **06** (2009) 018 [arXiv:0903.1481] [INSPIRE].

[24] A.D. Linde, *Inflation and string cosmology*, *Prog. Theor. Phys. Suppl.* **163** (2006) 295 [hep-th/0503195] [INSPIRE].

[25] R. Kallosh, *On inflation in string theory*, *Lect. Notes Phys.* **738** (2008) 119 [hep-th/0702059] [INSPIRE].

[26] A. Ashoorioon and M.M. Sheikh-Jabbari, *Gauged M-flation, its UV sensitivity and Spectator Species*, *JCAP* **06** (2011) 014 [arXiv:1101.0048] [INSPIRE].

[27] A. Ashoorioon, H. Firouzjahi and M.M. Sheikh-Jabbari, *Matrix Inflation and the Landscape of its Potential*, *JCAP* **05** (2010) 002 [arXiv:0911.4284] [INSPIRE].

[28] Z. Huang, *The Art of Lattice and Gravity Waves from Preheating*, *Phys. Rev.* **D 83** (2011) 123509 [arXiv:1102.0227] [INSPIRE].

[29] C.P. Burgess, M. Cicoli and F. Quevedo, *String Inflation After Planck 2013*, *JCAP* **11** (2013) 003 [arXiv:1306.3512] [INSPIRE].

[30] K. Dasgupta, M.M. Sheikh-Jabbari and M. Van Raamsdonk, *Matrix perturbation theory for M-theory on a PP wave*, *JHEP* **05** (2002) 056 [hep-th/0205185] [INSPIRE].

[31] A.A. Abolhasani, H. Firouzjahi and M.M. Sheikh-Jabbari, *Tachyonic Resonance Preheating in Expanding Universe*, *Phys. Rev.* **D 81** (2010) 043524 [arXiv:0912.1021] [INSPIRE].

JCAP03(2014)020

[32] N.W. Mac Lachlan, *Theory and Application of Mathieu Functions*, Dover Publications, New York, U.S.A. (1961).

[33] L.D. Landau and L. Lifshits, *Mechanics*, Pergamon Press, New York, U.S.A. (1976).

[34] L.D. Landau and L. Lifshits, *The classical theory of fields*, Pergamon Press, New York, U.S.A. (1976).

[35] J. Giblin, T. John, L.R. Price and X. Siemens, *Gravitational Radiation from Preheating with Many Fields*, *JCAP* **08** (2010) 012 [arXiv:1006.0935] [INSPIRE].

[36] Private communications with Zhiqi Huang.

[37] A.M. Cruise, *An interaction between gravitational and electromagnetic waves*, *Mon. Not. Roy. Astron. Soc.* **204** (1983) 485.

[38] A.M. Cruise, *An electromagnetic detector for very-high-frequency gravitational waves*, *Class. Quant. Grav.* **17** (2000) 2525 [INSPIRE].

[39] A.M. Cruise and R.M.J. Ingley, *A prototype gravitational wave detector for 100 MHz*, *Class. Quant. Grav.* **23** (2006) 6185 [INSPIRE].

[40] F.-Y. Li, M.-X. Tang and D.-P. Shi, *Electromagnetic response of a Gaussian beam to high frequency relic gravitational waves in quintessential inflationary models*, *Phys. Rev.* **D 67** (2003) 104008 [gr-qc/0306092] [INSPIRE].

[41] M.-l. Tong, Y. Zhang and F.-Y. Li, *Using polarized maser to detect high-frequency relic gravitational waves*, *Phys. Rev.* **D 78** (2008) 024041 [arXiv:0807.0885] [INSPIRE].

JCAP03(2014)020